A Mutation Affecting Basal Body Duplication and Cell Shape in *Paramecium*

F. Ruiz, N. Garreau de Loubresse,* and J. Beisson

Centre de Génétique Moléculaire du Centre National de la Recherche Scientifique, Gif-sur-Yvette, France; and
*Centre de Biologie Cellulaire du Centre National de la Recherche Scientifique, Ivry-sur-Seine, France

Abstract. The thermosensitive mutant *sml9* of *Paramecium tetraurelia* undergoes a progressive reduction in cell length and basal body number over successive divisions at the nonpermissive temperature of 35°C. In spite of these defects, *sml9* cells retain the same generation time as wild-type cells at 35°C. Cytological observations at both electron and light microscopy levels reveal no other perturbation than the rarefaction of basal bodies and the rare (3%) absence of one or two microtubules in basal bodies or ciliary axonemes. The temperature-sensitive period, during the last 30 min of the cell cycle, corresponds to the phase of basal body duplication. Upon transfer back to the permissive temperature, all basal bodies are normally duplicated. The mutational defect is transiently restored by microinjection of wild-type cytoplasm or of a soluble proteic fraction from wild-type cell homogenates. Altogether, the cytological and physiological data support the conclusion that the *sml9*$^+$ gene codes for a diffusible product required for the initiation of basal body duplication and would thus be the first identified gene involved in this process. Our data also indicate that in *Paramecium* basal body number is not coupled with control of the cell cycle, but helps determine the shape of the cell via the organization of the cytoskeleton.

THE basal bodies of ciliates and flagellates duplicate in the same way as centrioles: each new basal body develops close to a preexisting one and at right angles to it. The factors that trigger duplication and the mechanisms that control the assembly of this ubiquitous eukaryotic structure are still unknown, but could, in principle, be genetically dissected provided that mutations blocking some step of the process could be phenotypically identified. Ciliates provide a favorable system for detection of defective basal body duplication, since their cortex is made of highly ordered cortical rows of regularly spaced basal bodies, easily observed under light microscopy. Mutants with reduced numbers of basal bodies have indeed already been described in *Paramecium* (26) and *Euplotes* (14). However, in none of these cases has it been established that the mutation primarily affected basal body duplication per se, rather than subsequent events involving the insertion of basal bodies in the plasma membrane.

We describe here a thermosensitive nuclear recessive mutation of *Paramecium tetraurelia*, *sml9*, which results, over successive divisions at the nonpermissive temperature, in a progressively decreasing number of basal bodies and a correlatively reduced cell length and modified cell shape. By following different cytological and physiological parameters (cell length, basal body number, cortical organization, ultrastructure, generation time, protein synthesis, and feeding activity), we have analyzed the expression of the mutation upon transfer of *sml9* cells to the nonpermissive temperature and their recovery after return to the permissive temperature. All the observations support the conclusion that the primary effect of the mutation affects basal body duplication. We have also demonstrated that the mutational defect can be repaired transiently by microinjection of soluble cytoplasmic factors of a proteinic nature. The results will be discussed in relation to the mechanisms of basal body duplication and to the role of basal body number in the control of the cell cycle and the determination of cell shape.

Materials and Methods

Strains and Culture Conditions

The wild-type strain used in these experiments and from which the mutant *sml9* was isolated was the stock d4-2 of *P. tetraurelia* (39). Depending on the experiments, the wild-type strain and the mutant expressed either one of the two complementary mating types, referred to as VII and VIII (38, 40). We also used the mutants *sm2* and *sm3* isolated from stock 51 of *P. tetraurelia* by Jones and Berger (26) and kindly provided by Dr. J. Berger, University of British Columbia, Vancouver, British Columbia, Canada. These two thermosensitive mutants are characterized by an abnormal cell shape and a reduced number of basal bodies at the nonpermissive temperature, 35°C. The mutation *nd7* (3, 40), which prevents trichocyst discharge, was used as a genetic marker in certain crosses.

Cells were grown at either 28 or 35°C in a grass infusion bacterized with *Aerobacter aerogenes* and supplemented with 0.4 μg/ml β-sitosterol.

Mutagenesis and Crosses

Mutagenesis was carried out with *N*-methyl,*N*'-nitro-*N*-nitrosoguanidine from Aldrich Chemical Co. at a final concentration of 75 μg/ml for 45 min

on exponentially growing cells competent for autogamy. After mutagenesis, autogamy was induced by starvation. This leads to the breakdown of the old macronucleus and to the formation of new micro- and macronuclei homozygous for all their genes, so that ex-autogamous cells can express the mutations that have been induced. In this experiment, 14,000 cells were isolated in 96-well plates as previously described (8) and all the clones were tested at 35°C by replica plating after 10 generations at 28°C. All the clones presenting morphological abnormalities were kept for further investigation.

Crosses were carried out according to the classical methods described by Sonneborn (39).

Synchronization of the Cells

From exponentially growing populations maintained at 28°C for 10 generations after a controlled autogamy, pools of 25 cells in the last stage of division were picked up and transferred into fresh medium at either 28°C or at the restrictive temperature (35°C) using slides and medium preincubated at the respective temperatures. Within each pool, all the cells completed their division within a 5-min interval, yielding a small population of synchronous cells at the time 0 of their next cell cycle. Members of a synchronous pool were either isolated or kept together in depression slides and periodically examined for observation of the successive divisions. At chosen times, cells were picked up and fixed for length measurements or cytological observations.

Measurements of the Cells

Measurement of cell length was chosen as the simplest and most significant parameter for the mutants studied. Cells were gathered in a drop of culture fluid and fixed by addition of a drop of Dippell's stain (11), a rapid technique previously shown to preserve the in vivo dimensions (Beisson, J., and M. Rossignol, unpublished observation). Length was measured with an ocular micrometer adapted on a Zeiss light microscope at low magnification without a coverslip. Depending on the experiment, cells were measured just after completion of division or 1 h later.

Cytological Techniques

Silver Impregnation. The method was essentially that of Chatton and Lwoff (7).

Immunocytological Methods. Immunodecoration of specific cortical structures was carried out using the Schliwa and van Blerkom method (37) adapted to *Paramecium* as described by Cohen et al. (9). Deciliation was obtained immediately before permeabilization treatment by two successive transfers into 10 mM $MnCl_2$ (15) until immobilization. The antitubulin antiserum used was that raised against *Paramecium* axonemal tubulin described by Cohen et al. (9). After permeabilization, cells were incubated for 1 h in the antiserum diluted 1/400, washed twice for 5 min, then incubated for 1 h in FITC-antirabbit antibodies diluted 1/200. Cells were rinsed twice, mounted in glycerol containing 2% *n*-propyl-gallate to reduce photobleaching of the fluorochromes (16), observed, and photographed under a Zeiss epifluorescent microscope.

Electron Microscopy. The cells were fixed in 2% glutaraldehyde in 0.05 M cacodylate buffer (pH 7.2) for 90 min at 4°C. After washing in the same buffer, the samples were postfixed in 1% osmium tetroxide in 0.05 M cacodylate for 60 min. The samples were then dehydrated by passage through a series of ethanol and propylene oxide baths and embedded in Epon. Thin sections were contrasted with ethanolic uranyl acetate and lead citrate, then examined with a Philips EM 201 electron microscope.

Scanning Electron Microscopy. The cells were quickly deciliated in $MnCl_2$ and fixed in 2% glutaraldehyde in 0.05 M cacodylate buffer, pH 7.2, for 30 min. In this medium, the cells were then attached to polylysine-treated coverslips (33) by centrifugation for 10 min at 3,000 rpm. After washing in 0.05 M cacodylate buffer, the attached cells were postfixed in 1% osmium tetroxide for 30 min in the same buffer and further dehydrated in a graded series of ethanol and acetone. The samples were dried at the critical point and examined with a Phillips 505 scanning electron microscope.

Observation of Food Vacuole Formation

One drop of India ink diluted 1/100 in distilled water was added to 1 ml cell populations in depression slides. Ingestion of ink particles strongly labels the food vacuoles (6). After 30 min, cells were fixed and the number of labeled food vacuoles per cell was counted under the light microscope.

Protein Measurement

Log phase cultures of wild type and *sml9* grown at the permissive temperature were transferred into medium preincubated at the nonpermissive temperature and maintained in log phase. At chosen times cultures were filtered. Cell density was determined by counting 1-ml aliquots of the populations, and the total volume of the cultures was measured. Cells were centrifuged in an oil centrifuge at 1,000 rpm for 2 min, then washed twice in a 10-mM Tris maleate buffer, pH 7.8. The cellular pellet, resuspended in 0.5 ml buffer, was transferred to an Eppendorf tube. After addition of SDS to a final concentration of 1%, samples were immediately boiled for 3 min, then centrifuged, and protein concentration determined on aliquots by the method of Lowry et al. (30) using bovine serum albumin as a standard. SDS was added to all controls.

Microinjection Technique

The technique used was that described by Knowles (28). The recipient cell was injected with either a small volume (~5,000 μm^3) of cytoplasm sucked out of the donor cell immediately before injection or with a similar volume of a soluble fraction prepared from cell homogenates. Injections were carried out at 18°C. Cells were transferred to the nonpermissive temperature 1 or 2 h after injection. Depending on the experiment, the percentage of survivors after transfer to 35°C ranged from 17 to 82%.

Cell Fractionation

Wild-type cells at the end of log phase were washed twice in 10 mM phosphate buffer, pH 7.0, and centrifuged. 1 vol of the cell pellet was mixed with 1 vol of buffer A (sucrose, 0.2 M; potassium phosphate, 50 mM, pH 7.0). The cells were homogenized in a Dounce homogenizer at 4°C, and first centrifuged at 30,000 *g* for 20 min. The supernatant was recentrifuged at 100,000 *g* for 1 h, yielding a postmicrosomal supernatant. This fraction was stored at −80°C. From the postmicrosomal supernatant, proteins were precipitated by 80% ammonium sulfate and the precipitate dialyzed extensively against buffer A. The samples were kept at −80°C.

Split-pair Experiments

During conjugation, paired paramecia remain united for 5–6 h at 28°C. The exchange of gametic nuclei, which will provide both partners with an identical heterozygous nuclear complement, occurs by the fourth hour. However, electrical coupling between conjugants is achieved by the first 1½ h and labeled amino acids and macromolecules diffuse from one conjugant to the other (31) long before nuclear exchanges, while it is still possible to force the conjugants to separate. This situation provides the rationale for the split-pair experiments. Sexually reactive *sml9* and wild-type cells of complementary mating type were mixed and 1½ h later, pairs of conjugants were forced to separate. Each exconjugant was then individually transferred to 35°C. Comparison with control *sml9* × *sml9* split pairs allowed us to determine whether the mutant phenotype had been restored by contact with a wild-type partner.

Results

The morphology of *P. tetraurelia* and the morphogenetic processes involved in its division have been extensively described (27). The most striking features of division concern the reproduction of the organization of the cell cortex and one of the key events lies in basal body duplication.

Wild-type *P. tetraurelia* was mutagenized with nitrosoguanidine and individual ex-autogamous (i.e., homozygous, see Materials and Methods) clones were screened for abnormal morphology expressed only at the nonpermissive temperature of 35°C. Mutant *sml9* was isolated on the basis of its reduced cell length and rounded shape at 35°C. Preliminary cytological observations revealed that the small cells also displayed a marked reduction in basal body number. In both respects, *sml9* resembled the mutants *sm2* and *sm3* previously described by Jones and Berger (26). This similarity led us to analyze various aspects of the mutant *sm2* in conjunction with our study of the mutant *sml9*.

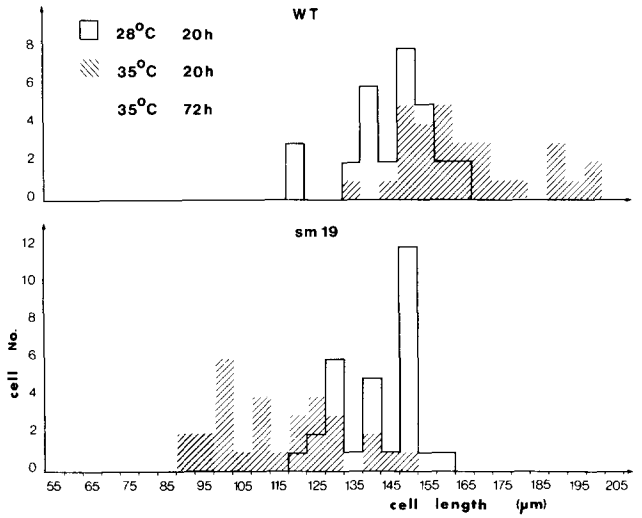

Figure 1. Comparison of the lengths of wild-type and *sml9* cells at 28 and 35°C. The histograms represent the distribution of the lengths of wild-type (WT) and *sml9* cells in samples of 30 cells taken from populations grown at 28 or 35°C. The upper histograms correspond to exponentially growing wild-type cells at 28 or 35°C. The lower histograms show the decrease in the lengths of *sml9* cells maintained at 35°C, as compared with their lengths at 28°C. Wild-type and mutant mean lengths were compared by calculation of the error on the estimation of the mean at a 5% risk level. The means are similar at 28°C (respectively, 146 ± 4 and 141 ± 4) while they are significantly different at 35° C (respectively 160 ± 6 for the wild type and 115 ± 6 after 20 h and 79 ± 5 by 72 h for the mutant).

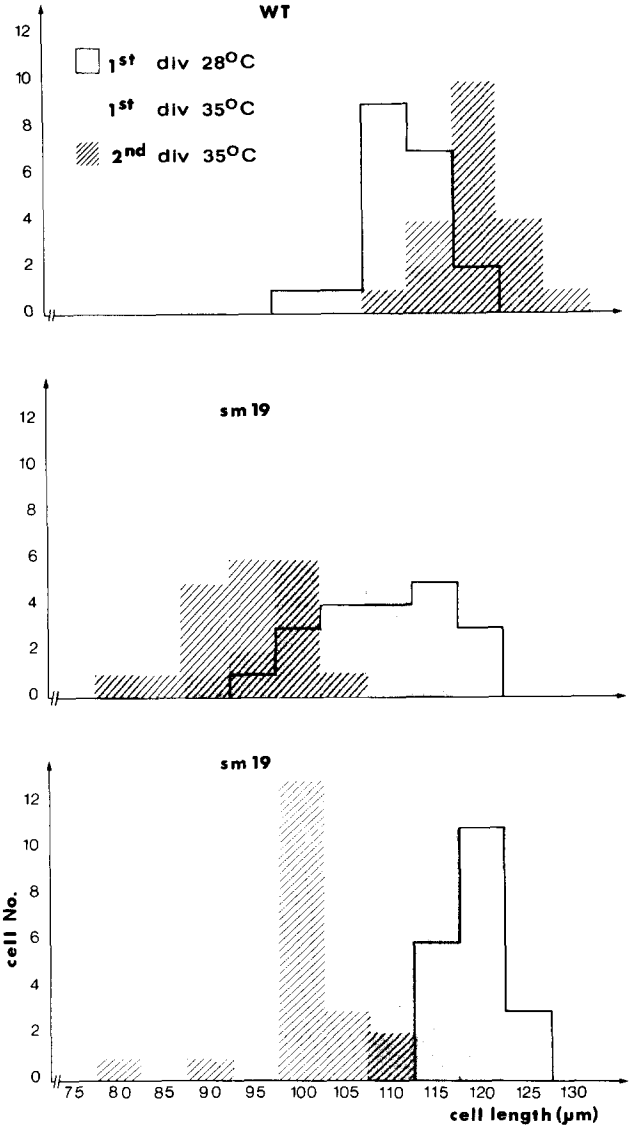

Figure 2. Comparison of the lengths of synchronized wild-type and *sml9* cells. Synchronized cells were either maintained at 28°C and measured at the end of one cycle or transferred to 35°C and measured after exactly one or two complete cycles at the nonpermissive temperature. The upper histogram compares the lengths of wild-type cells at the two temperatures. The lower two histograms present the results for two different experiments with the mutant. Mean cell lengths (and the error on the estimation of the mean at a 5% risk level) at 28°C and after one and two divisions at 35°C were, respectively, 112 ± 2, 117 ± 4, and 120 ± 2 for wild type; and 109 ± 2, 102 ± 3, and 94 ± 2 (middle histogram) and 119 ± 2, 113 ± 2, and 100 ± 3 (lower histogram) for *sml9*.

Genetic Analysis

The mutant clone *sml9* was crossed with the wild-type strain. All F1 clones were of wild-type phenotype, and after autogamy of the F1 clones, an F2 ratio of 48 *sml9*$^+$/57 *sml9* clones was obtained. *sml9* was also crossed with a strain of wild-type morphology and growth, carrying the trichocyst nondischarge mutation *nd7* (2, 40), yielding an F2 segregation of 17 *sml9 nd7*$^+$/15 *sml9 nd7*/15 *sml9*$^+$*nd7*/11 *sml9*$^+$*nd7*$^+$. These results showed that *sml9* phenotype corresponded to a single nuclear recessive mutation, independent of *nd7*.

The mutant *sml9* was then crossed with the mutants *sm2* and *sm3*. In both crosses, the F1 clones displayed wild-type phenotypes, and in the F2, the *sml9* mutation segregated independently of the *sm2* and *sm3* mutations.

Double mutants recovered from the F2 of these crosses were studied. While no interaction between the *sm3* and *sml9* mutations were detected (their phenotypes being indistinguishable from that of either parent), a synergy between the mutations *sml9* and *sm2* was observed. The double mutants displayed more pronounced morphological abnormalities at the nonpermissive temperature than either parent.

Phenotypic Analysis

Cell Size and Shape. Fig. 1 compares the distribution of cell lengths in wild-type and *sml9* populations at permissive (28°C) and nonpermissive (35°C) temperatures. At 28°C, the size distribution of both wild-type and mutant cells is identical. After 20 h at 35°C, while the populations are still in log phase, the size of wild-type cells slightly increases, as previously described by Whitson (41); in contrast, the mean length of *sml9* cells is reduced (to 71% of the initial value) and the distribution of lengths is more heterogeneous. This phenomenon was studied more precisely using synchronous populations (see Materials and Methods). Fig. 2 shows for *sml9* cells a progressive significant decrease in mean cell length of 6–7% by the first division and 14–16% by the second one. Fig. 3 illustrates the correlative change in cell shape after three to four divisions at 35°C; the cells are not only shorter but much less tapered at the poles.

Generation Time. Pools of cells that have just divided retain their synchrony over a few generations, and, as illustrated in Fig. 4, display sharp peaks of division that provide

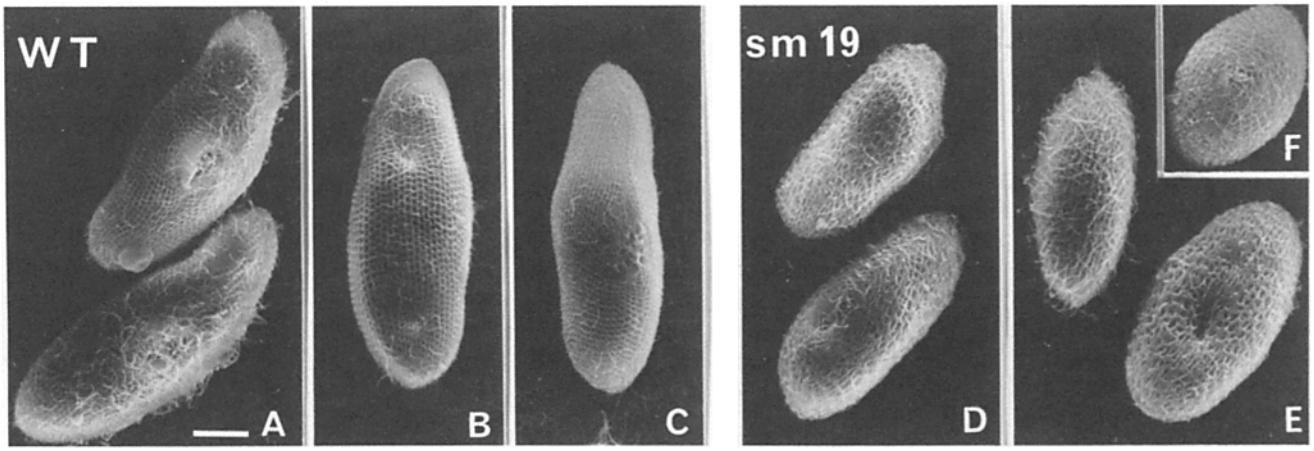

Figure 3. Evolution of the shape of *sml9* cells at 35°C. At 27°C, both wild-type and mutant cells display identical size and shape. Despite a slight increase in length, the shape of wild-type cells grown at 35°C is identical to that of cells grown at 27°C. Populations of wild-type (*A–C*) and *sml9* cells (*D–F*) grown for 20 h at 35°C were prepared for scanning electron microscopy. A sample of cells taken from each preparation is shown here. The reduced length and modified shape of the mutant cells are apparent. The extent of deciliation was variable from cell to cell for both populations. Bar, 10 μm.

a good estimate of the generation time. However, for unknown reasons, the absolute values measured for generation time vary. For both wild-type and *sml9* cells, the values were found to range, in many different experiments, from 5 to 7 h at 28°C, from 4 to 4½ h for the first division at 35°C, and from 3½ to 4 h for subsequent divisions at 35°C. Within these limits of variation, Fig. 4 shows that *sml9* cells maintain the same generation time as wild-type cells upon transfer to 35°C, as consistently observed in many other experiments not followed beyond the second division at 35°C. In contrast, in similar experiments, the mutant *sm2* (whose growth rate at 28°C is identical to that of wild-type cells) displayed a generation time of 5 to 6.5 h for the first division at 35°C, and the longer generation time was accompanied by a significantly decreased synchrony.

Cortical Organization. The cortex of *Paramecium* is characterized (*a*) by the alignment of parallel rows (kineties) of regularly spaced basal bodies (and cilia); (*b*) at the whole cell level, by a precise asymmetrical arrangement of kineties and (*c*) by the complex structure of the ingestatory apparatus, the gullet, a funnel-shaped invagination where several hundred basal bodies (and cilia) form three groups of four parallel rows. During division, the reconstruction of this organization is accomplished on both sides of the equatorial fission furrow by proliferation of new basal bodies. As described by Dippell (12), each new basal body is precisely positioned along the kinety axis, anteriorly with respect to the mother basal body, thus ensuring the perpetuation of the kinety pattern. The old gullet is transmitted in its entirety to the anterior fission product, while a new one, progressively assembled from an anarchic field of proliferating kinetosomes (24) on the right margin of the old gullet, migrates during division into the posterior fission product.

Basal bodies were visualized by two techniques, classical silver impregnation and decoration by an antitubulin antiserum (see Materials and Methods). While the first technique only reveals basal bodies positioned at the surface, the second can also reveal newly formed basal bodies still below the plasma membrane. As shown in Figs. 5 and 6, respectively,

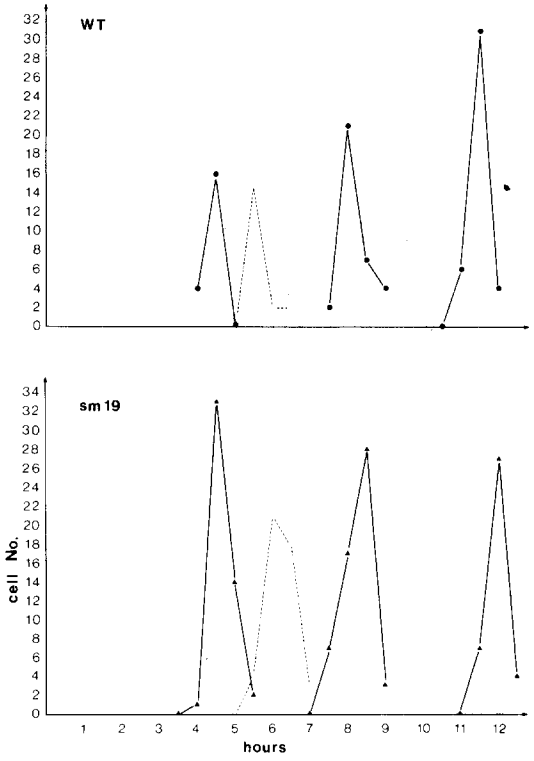

Figure 4. Successive cell cycles of wild-type and *sml9* cells over three successive divisions at 35°C. Synchronized cells were either maintained at 28°C or transferred to 35°C and periodically observed in order to record the number of cells undergoing division. This number is plotted against time. The peaks show that good synchrony is retained and provide an estimate of the generation time at 28°C as well as over the successive cycles at 35°C. For instance, these generation times can be estimated to be, for the *sml9* cells, 6 h at 28°C and, successively, 4½, 4, and 4 h at 35°C. (*Dotted lines*) Divisions at 28°C; (*solid lines*) divisions at 35°C.

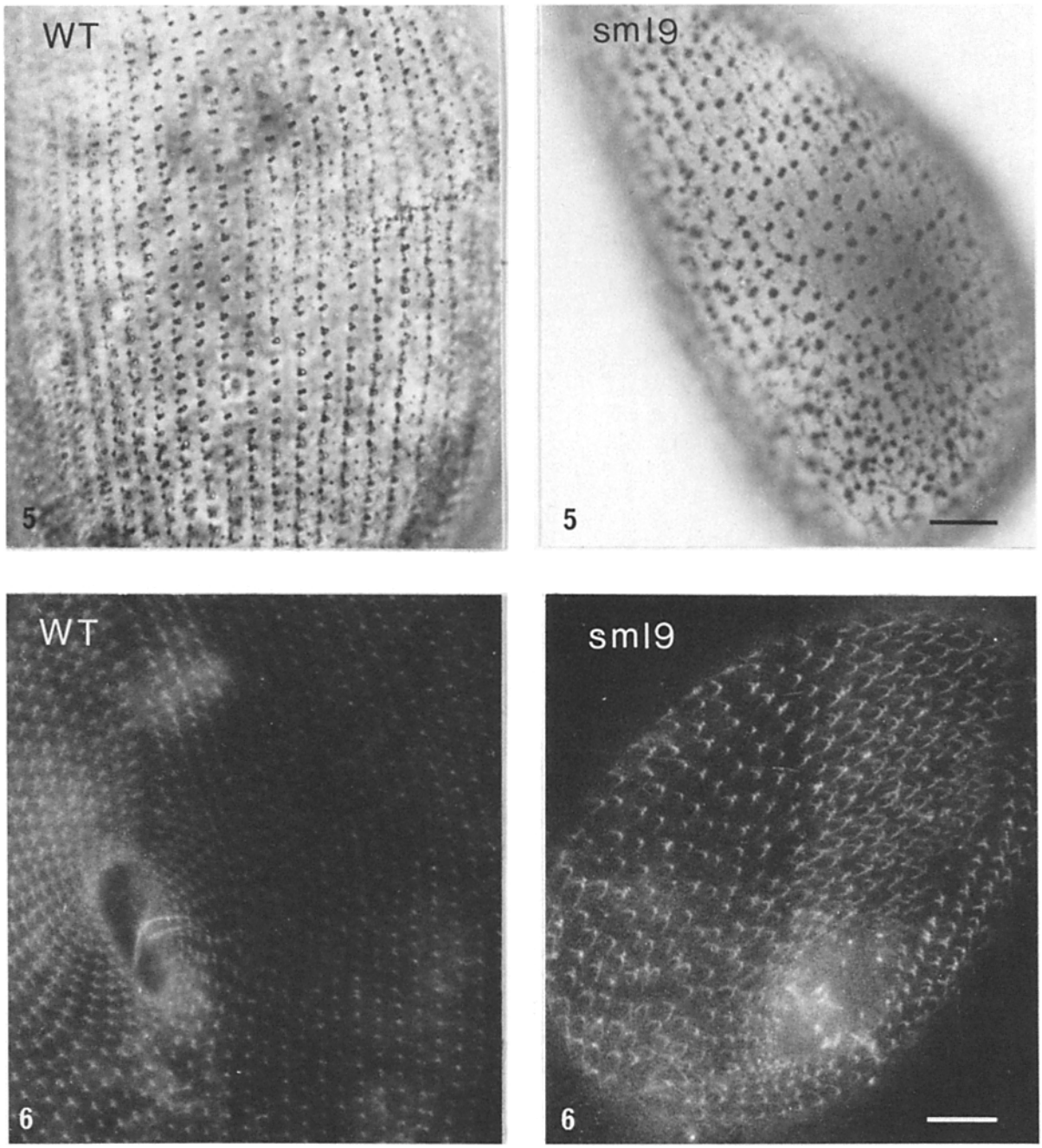

Figures 5 and 6. Cortical disorders in *sml9* cells after several divisions at 35°C. The rarefaction of basal bodies and the overall reduction of cell size is apparent. (Fig. 5) Silver-impregnated wild-type (*WT*) and *sml9* cells. Bar, 10 μm. (Fig. 6) WT and *sml9* cells decorated with the antitubulin antiserum, showing basal bodies and their posterior and transverse microtubule ribbons. Bar, 10 μm.

the two techniques demonstrate a reduction in the number of basal bodies per cell and wider spacing between basal bodies in *sml9* cells grown at 35°C.

A reduction in the number of basal bodies is also detected in the neoformed gullet by the first division at 35°C (Fig. 7). Although not always conspicuous, such abnormalities develop in all neoformed gullets. Among 61 cells examined after the first division at 35°C, 25 (presumably posterior fission products) showed a clearly abnormal gullet, while 36 displayed an apparently normal one. The number of basal bodies continues to decrease over the next division. This deficiency is accompanied by a progressive disorganization of the gullet, which in turn impairs the feeding activity so that *sml9* cells die of starvation after four to six divisions at 35°C.

That this rarefaction of basal bodies in the cortex and in the gullet is indeed due to a defective duplication of the organelle is demonstrated by two observations. (*a*) Basal body duplication, mostly achieved before cells enter division, follows a precise pattern, and at predivision or early division stages newly formed basal bodies can be unambiguously identified. In particular, on both sides of the fission furrow,

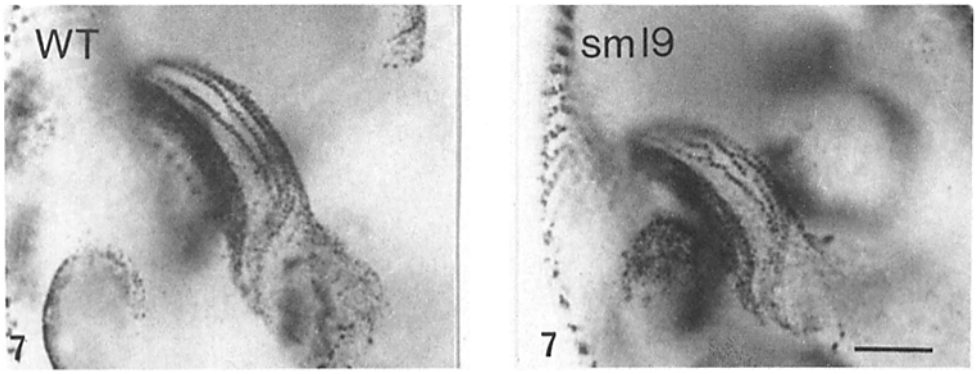

Figure 7. Disorganization of the gullet in *sml9* cells after one division at 35°C. In these silver-impregnated cells, the picture is focused on the center of the gullet. In the mutant *sml9*, basal bodies are sparser along each row and the rows are disorganized. Bar, 10 μm.

each preexisting basal body generates two or three new ones, yielding files of three or four basal bodies, easily visible using either silver impregnation or antitubulin staining. With both techniques, *sml9* cells fixed during their first division at 35°C (as well as during subsequent ones) display a significantly reduced number of newly formed basal bodies. (*b*) During sexual processes, autogamy, or conjugation, the gullet is resorbed and a new one generated by a proliferation of basal bodies, which in this case is not accompanied by cell growth or multiplication of cortical basal bodies. *sml9* × *sml9* couples of conjugants, grown and crossed at 27°C and transferred to 35°C, displayed, after separation of the conjugants and before any further division, the same abnormalities and reduction of basal body number in their gullet as those illustrated in Fig. 7.

The progressive reduction in basal body number was the sole defect detected in cells decorated by the antitubulin antiserum. Even after several divisions at 35°C, none of the various transient (nuclear spindles, cytospindle), semipermanent (post oral fibers, intracytoplasmic network), or permanent microtubule arrays previously described by Cohen et al. (9) were affected, except for an increased length, apparently adjusted to the wider spacing of basal bodies, of the transverse and post ciliary ribbons nucleated on each basal body (Fig. 6). These observations suggest that tubulin availability is probably not the limiting factor responsible for basal body loss.

Kinetics of Basal Body Loss. Counting basal bodies (on silver nitrate or antitubulin-decorated preparations) raises practical difficulties. As basal bodies can only be counted on the flattened parts of the cells and not around the poles or at the periphery, we did not attempt to determine their total number and chose to limit counting to selected areas of the cell surface. However, basal body density (i.e., number per surface unit) varies from region to region, and, furthermore, varies for a given region throughout the cell cycle, owing to surface and volume increase during the interphasic period and to profound shape remodeling during division when basal bodies proliferate neither synchronously nor equally in the different regions. Finally, basal bodies had to be counted after exactly one, two, and three cycles at 35°C on synchronized cells, so that only small samples of cells could be prepared. Not all of the cells among these presented a favorable view of the selected regions.

An estimate of basal body loss in *sml9* cells grown at 35°C was obtained by comparing their number with that of the corresponding regions in wild-type cells in two ways: (*a*) counting the total number of basal bodies along the same middorsal kinety on preparations such as those illustrated in Fig. 5; and (*b*) counting the number of basal bodies within an ar-

Table I. Loss of Basal Bodies in sml9 Cells Grown at 35°C

	WT 28°C		sml9 28°C		WT 35°C(1)		sml9 35°C(1)		sml9 35°C(2)		sml9 35°C(3)	
	No. of cells	Mean bb No.	No. of cells	Mean bb No.	No. of cells	Mean bb No.	No. of cells	Mean bb No.	No. of cells	Mean bb No.	No. of cells	Mean bb No.
A	4	65 (64–66)	10	66 (63–69)	5	68 (67–70)	13	51 (47–58)	11	41 (34–42)	8	33 (27–38)
B					15	35 (28–48)	22	32 (21–40)	14	23 (18–28)	14	24 (19–29)
C					11	66 (59–72)	12	51 (43–58)	11	33 (26–31)		
D					10	43 (35–55)	11	38 (29–48)	8	33 (26–40)		
B + C + D						144		121		89		

Loss of basal bodies (bb) in *sml9* cells over the first three divisions at 35°C. Basal body number was counted on selected areas of *sml9* cells at 28°C and after one, two, and three divisions at 35°C and compared with basal body number in similar areas of wild-type cells under similar conditions. Four types of counts were carried out. (A) Total number of basal bodies along the same middorsal kinety. (B–D) Number of basal bodies within a 100-μm² area respectively located in the middle of the dorsal side (B), in the left (C), and right (D) sides of the posterior suture (ventral side), just below the posterior edge of the gullet opening. In each case we indicate the number of cells examined, the mean basal body number, and, in parenthesis, the extreme observed values. All counts were made on synchronous cells fixed at either 28°C or after exactly one division (*sml9*[1]), two divisions (*sml9*[2]), or three (*sml9*[3]) divisions at 35°C.

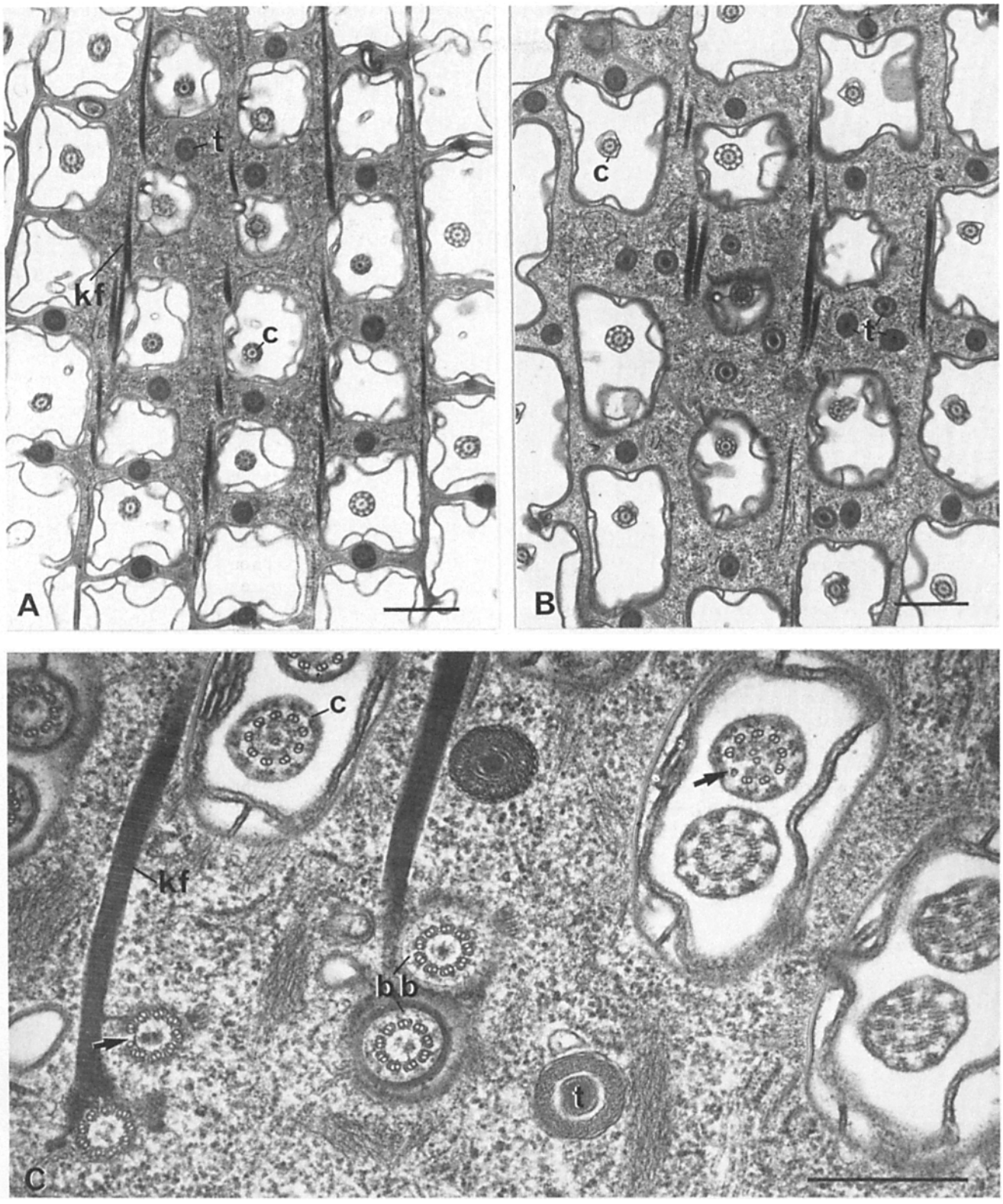

Figure 8. Cross sections tangential to the surface of wild-type (*A*) and *sml9* cells (*B* and *C*). Cells were fixed after four to five divisions at 35°C. (*A* and *B*) In the mutant, the rarefaction of basal bodies and correlative enlargement of cortical units and mispositioning of trichocysts is apparent. (*C*) A more oblique tangential cross section through both cilium and basal body levels showing missing microtubules in both cilia and basal bodies (*arrows*). (*bb*) Basal body; (*c*) cilium; (*kf*) kinetodesmal fiber; (*t*) trichocyst tip. Bars (*A* and *B*), 1 μm; (*C*) 0.5 μm.

bitrary surface (100 μm^2) in three regions: ventral posterior right, ventral posterior left, and middorsal. The data, presented in Table I, call for the following remarks. Since all cells present approximately the same number of basal bodies, one can assume that before each division, basal body number globally doubles and that each daughter cell inherits half of this doubled number. The global probability (k) of basal body duplication in the mutant can therefore be deduced from the number (n) of basal bodies at 28°C and the number (n') after one division at 35°C: $2n' = n + nk$. However, depending on the regions of the cortex, basal body density varies and basal bodies either do not duplicate or undergo one, or, near the equator, two cycles of duplication. While counts of basal bodies along a whole kinety integrate these regional variations, counts over particular surfaces (Table I, B–D) are more biased and need to be randomized in order to calculate the overall loss of basal bodies. The data show that, for the whole middorsal kinety (Table I, A) k = 0.6 for the first division and remains 0.6 for the next two divisions. The same coefficient also accounts for the global loss of basal bodies in different cell surface areas, summed up as B + C + D in Table I.

Ultrastructural Features. The organization of *sml9* cells (after three to four divisions at 35°C) was examined by electron microscopy. Fig. 8, *A* and *B* shows thin sections tangential to the cell surface of wild-type and *sml9* cells. The wider spacing of basal bodies is apparent. Rare abnormalities of a single type in the organization of basal bodies or cilia were detected (Fig. 8 *C*): missing microtubules among the nine outer doublets (or triplets, in the case of basal bodies). This defect was observed in 35 out of 1,143 sections of cilia or basal bodies from a total of 15 different cells. Strikingly, the defect was most often located in the right posterior part of the basal body or cilium. This was the case in 18 out of the 25 cases where the polarity of the basal body or cilium could be ascertained. Fig. 9 shows that this region corresponds to the site where, according to Dippell (12), the first tubule of the initial ring of nine singlets that initiates the development of a new basal body is nucleated.

Similar defects were also found in the double mutant *sm2 sml9* (not shown) but not in the mutant *sm2*. In contrast, Fig. 10 shows that *sm2* cells display distinctive ultrastructural abnormalities that are not shared by the mutant *sml9*: an excess of parasomal sacs (coated pits) and/or subcortical coated or uncoated vesicles and dilation of rough endoplasmic reticulum vesicles. An abnormal aspect of cortical membranes and an excess of cortical units containing two basal bodies were also observed (data not shown). The latter feature was confirmed by the fact that antitubulin-decorated *sm2* cells displayed more basal bodies than silver-stained cells, suggesting that the mutation *sm2* affects basal body positioning at the cell surface but not basal body duplication.

Determination of the Temperature-sensitive Period

As shown in Fig. 2, the mutation *sml9* is expressed by the first division in cells that have accomplished a complete cycle at 35°C, as judged by the 6–7% reduction in mean cell length. To define at which particular stage of the cell cycle the mutated gene exerts its phenotypic effect, synchronous cells were transferred from 28 to 35°C at different ages along their division cycle: 3 h, 4 h, etc., the latest time corresponding to half an hour or less before division at 28°C. Later shifts could not be carried out as the cells were not strictly synchronous and entered division over a 15–20-min interval. Cells completed their cycle at 35°C and were measured 1 h after division. Fig. 11 presents a representative example of several experiments and shows that in all cases the cells display a mean length characteristic of cells grown at 35°C for a complete cycle. The thermosensitive step takes place during the last 30 min of the cell cycle, which corresponds to the period of duplication of basal bodies (5, 12, 27).

It must be pointed out that our results integrate the effect of the nonpermissive temperature on both the last 20–30 min of the cell cycle (when basal bodies duplicate) and the first hour of the cell cycle (when cell length increases without further significant basal body multiplication). However, this protocol, chosen for experimental conveniency, does not impair the validity of our conclusions. First, in other temperature shift experiments (data not shown), *sml9* cells, exposed to 35°C for exactly 1 h after division at 28°C, displayed the same length as the control *sml9* cells kept at 27°C. Second, the observed length reduction is identical (~6–7%) in the ex-

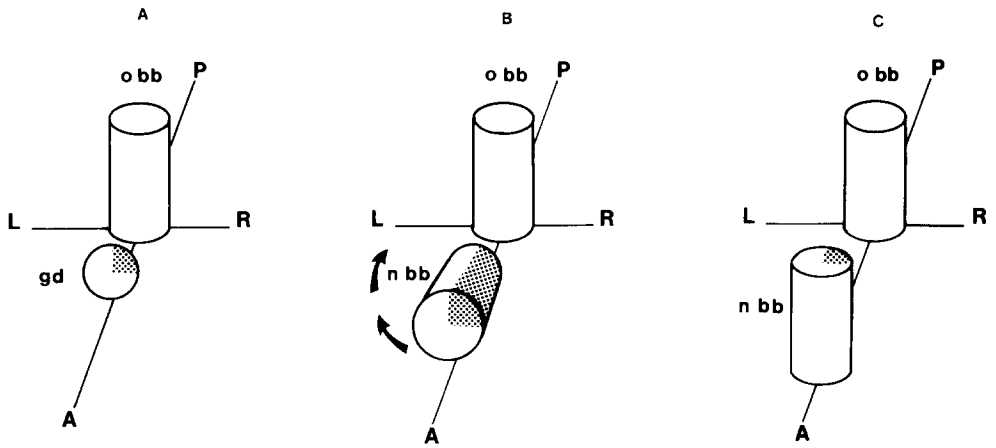

Figure 9. Development of a new basal body. As described by Dippell (12), a new basal body (*nbb*) develops from a germinative disc (*gd*) of electron-dense material located anterior to the old basal body (*obb*) along the anteroposterior cell axis. All basal bodies display an anteroposterior (*A–P*) and right–left (*R–L*) polarity defined, in particular, by their kinetodesmal fiber, emanating from the right side of the basal body and running towards the anterior of the cell. Microtubules are nucleated within the germinative disc, and grow perpendicularly to the old basal body, away from it. (*A*) According to Dippell (loc cit), the first microtubule is nucleated in the upper right of the germinative disc (*dotted sector*). (*B*) The new basal body elongates. (*C*) The new basal body tilts up to reach the surface and becomes parallel to the old basal body, along the axis of the kinety. The scheme shows that the posterior right part of a mature basal body corresponds to the upper right sector of its germinative disc.

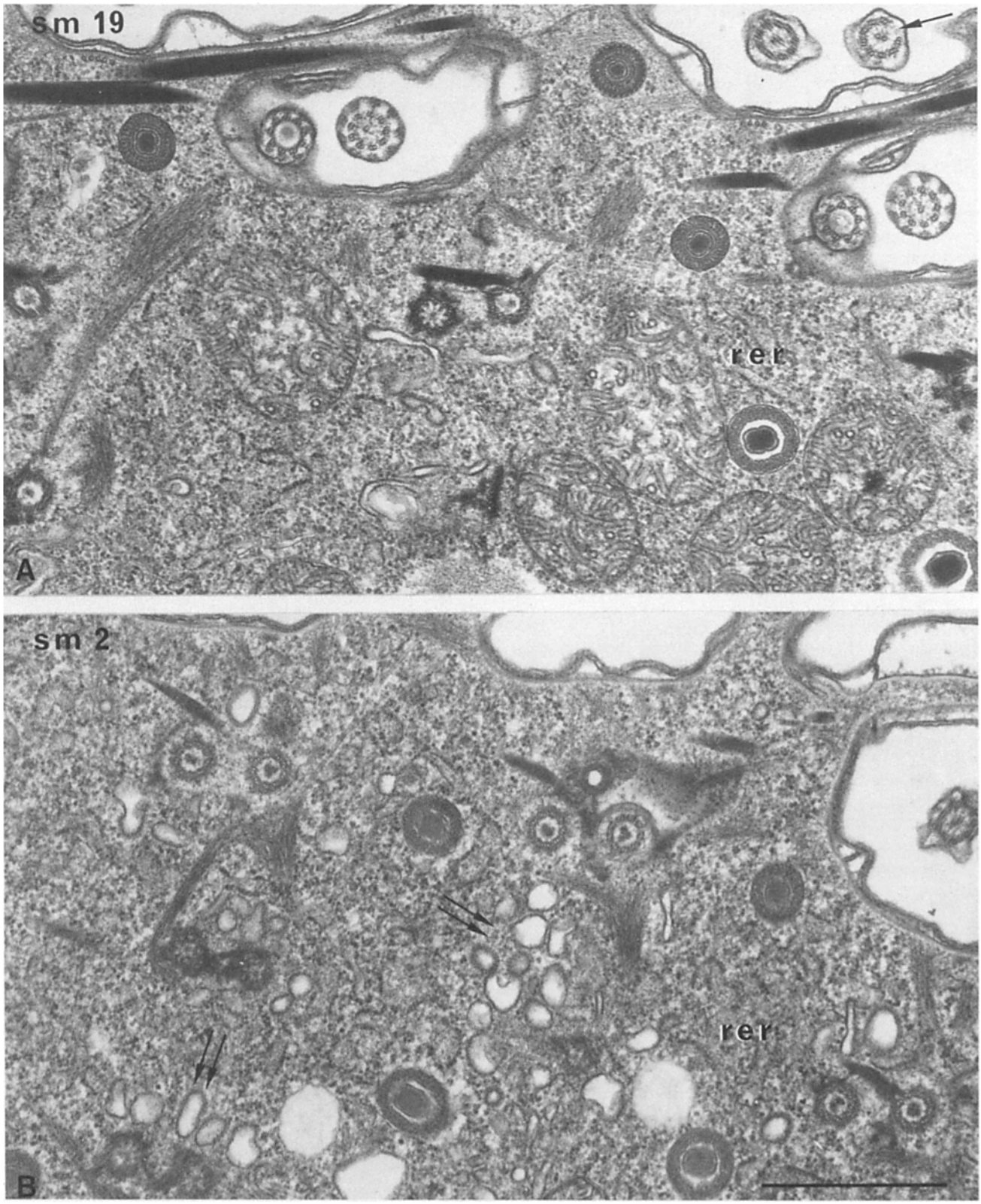

Figure 10. Thin sections through *sm19* (*A*) and *sm2* (*B*) cells. (*A*) The arrow shows another example of missing microtubules in a ciliary axoneme. (*B*) Two types of ultrastructural abnormalities of *sm2* cells are visible: excess of cortical or subcortical coated or uncoated vesicles (*double arrow*); and enlargement of rough endoplasmic reticulum (*rer*) cisternae. Bar, 1 μm.

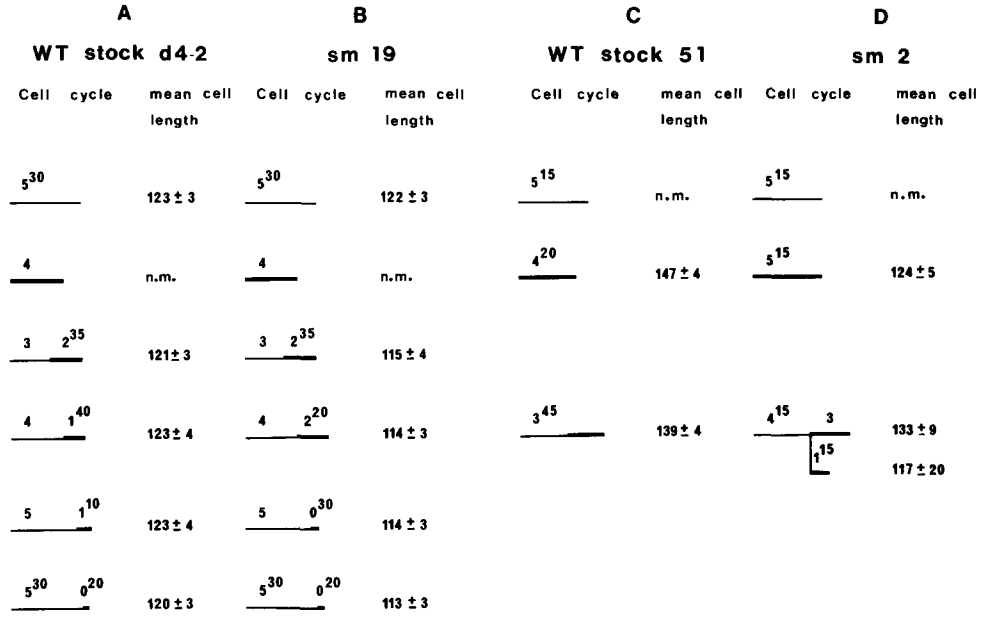

Figure 11. Determination of the temperature-sensitive period. Pools of synchronous wild-type and mutant cells grown at 28°C were transferred to 35°C at different times along their cycle at 28°C: 3 h, 4 h, etc., and divided (generally synchronously) after an additional time, as indicated on the figure. Their time of division at 35°C could be differently delayed, from pool to pool, by the heat shock. Nevertheless, within each pool, the cells generally retained their synchrony, except in the case of the mutant *sm2*, which often displayed two well-separated peaks of division, for instance at 1¼ and 3 h after the temperature shift in the experiment reported here. Whatever their behavior, cells were measured 1 h after the observed peak of division at 35°C. For a control, one pool was maintained at 28°C and cell lengths were also measured 1 h after division. The data on *sml9* and *sm2* were obtained in two different experiments. In each experiment the corresponding wild-type control was studied in parallel with the mutant. Mean cell length (and the error on the estimation of the mean calculated at a 5% risk level) is in micrometers. Thin line, time at 28°C; thick line, time at 35°C; n.m., not measured in these particular experiments.

periments reported in Fig. 2 (measurements made immediately after completion of division) and in those presented in Fig. 11.

In contrast, the results of the same temperature shift on *sm2* cells are more complex, since cell length may be greater for longer exposures to 35°C. Using a different protocol, Jones (25) demonstrated the existence of two sensitive periods, one extending from 0.35 to 0.65 of the cell cycle of *sm2* cells, and another one at ~0.85. Our observations, although they do not provide a simple explanation of *sm2* cell response to temperature shift, at least show that the two mutants respond differently.

Physiological Analysis

Since *sml9* cells maintain a normal generation time despite decreasing cell length and reduced basal body number, it seemed worthwhile to determine the protein content of *sml9* cells at 35°C and their capacity to synthesize tubulin, a major component of basal bodies. At least for the first two to three cell generations, the protein content of *sml9* cells was found to be identical to that of wild-type cells grown at 35°C = 16 ± 2 ng/cell. However, the protein content dropped to 9 ± 2 ng/cell beyond the third cell cycle, i.e., when the feeding capacity of the mutant cells began to decrease dramatically, as shown by the number of food vacuoles per cell (see Materials and Methods).

As for tubulin content and synthesis capacity, it was estimated to be identical to that of wild-type cells as judged by the speed and efficiency of reciliation of *sml9* cells deciliated (36) during their second cycle at 35°C. Deciliation did not reduce cell length in comparison with control undeciliated *sml9* cells.

Recovery after Shift Down to the Permissive Temperature

The progressive disorganization of the gullet results in the irreversible loss of feeding capacity. By monitoring food vacuole formation (see Materials and Methods), it was indeed observed that beyond four divisions at 35°C, a majority of the cells did not form any food vacuoles and died even if transferred back to 28°C. In contrast, all cells still capable of feeding divided at the same rate as wild-type cells when transferred to the permissive temperature. After the first division at 28°C, all these cells recovered a much more normal morphology. Furthermore, basal body spacing along each kinety was returned to normal (~1.5 μm) in most parts of the cell, indicating a general recovery of the basal body duplication pattern. However, most cells retained a smaller length. For instance, the mean cell length among clones issued from cells transferred to 28°C after four divisions at 35°C and measured after 7–8 fissions at 28°C could be as small as 74–84 μm. Six rescued clones were followed for 100–200 cell generations. Although some clones did not differ much from the control ones and despite the intraclonal variance, all six clones retained a statistically significant reduced length (data not shown).

These observations lead to several conclusions. (*a*) The immediate reduction in basal body spacing suggests that the basal bodies formed during previous divisions at 35°C were not permanently impaired in their duplication capacity. (*b*) In contrast, the long lasting reduced cell length (i.e., total number of basal bodies) suggests that, in spite of some overall regulation, the absolute number of basal bodies at generation *n* is strongly dependent upon the number at generation *n*-1, as can be expected from their conservative mode of

Table II. Microinjection of Wild-type Cytoplasm into sm19 Cells

Cells	Treatment	No. of clones tested	Mean length ≥125
sm19			
	Uninjected	23	0
	Injected with oil	5	0
	Injected with sm19 cytoplasm	8	0
	Donor of cytoplasm	11	0
	Injected with wild-type cytoplasm	25	8
WT			
	Uninjected	20	20
	Injected with sm19 cytoplasm	2	2

sm19 cells grown at 28°C and injected with wild-type cytoplasm were placed at 35°C. For each clone issued from the injected cells, cell length was measured after three to four divisions at the nonpermissive temperature. Various controls were examined. The figures represent, for each series, the total number of clones studied and the number of clones whose mean length was superior to 125 μm, i.e., significantly larger than the mean length of untreated *sm19* cells.

duplication. This result provides a new example of cortical inheritance (2). (*c*) As a consequence, it appears that cell length is partly dependent upon basal body number. (*d*) The fast recovery of a normal shape, correlated with the reduction of basal body spacing, indicates that cell shape is dependent upon the density of basal bodies rather than their absolute number.

Restoration of the sm19 Mutational Defect by Wild-type Cytoplasmic Diffusible Factors

As the mutation *sm19* is recessive, it was of interest to examine whether the mutational defect could be at least transiently repaired by wild-type cytoplasm. Two methods were employed: microinjection of wild-type cytoplasm into *sm19* cells and cell contact during conjugation with a wild type partner. The first technique had been successfully applied to the study of trichocyst mutations (1). The second technique (see Materials and Methods) had previously been used to demonstrate the reparability, through membrane contact and diffusion of cytoplasmic components, of the mutations *pwA* (4) and *nd9* (3) in *P. tetraurelia* and *cnrC* in *Paramecium caudatum* (19).

In both types of experiments, *sm19* cells grown at 28°C were transferred to 35°C after microinjection or interrupted pairing and the clones issued from the treated cells were compared with those derived from control *sm19* cells. Depending on the experiments, different parameters were used to estimate the restoration of the *sm19* phenotype (mean cell length or number of divisions and feeding activity after 48 h). Table II indicates that 8 out of 25 *sm19* cells injected with wild-type cytoplasm retained, after three to four divisions at 35°C, a wild-type mean length. The data of Table III show that, in split-pair experiments, the contact with a wild-type partner induced a significant delay in expression of the *sm19* defect in more than half of the treated cells, since after approximately nine divisions more than half of the cells retained a normal morphology and feeding capacity. In contrast, no restoration by cell contact was observed for the *sm2* mutation.

Efficient rescue of the *sm19* phenotype was also obtained by microinjection of a postmicrosomal supernatant prepared from homogenates of wild-type cells and the $(NH_4)^2SO_4$-precipitated fraction of the postmicrosomal supernatant. In the latter case, out of 39 injected *sm19* cells (and 32 surviving ones), 20 yielded transiently restored clones on the basis of either cell mean length or the number of divisions and feeding activity at 35°C. These preliminary results suggest that the restoring factor is a soluble protein that most likely corresponds to the product of the gene $sm19^+$.

Discussion

Upon transfer to the nonpermissive temperature (35°C), the mutant cells *sm19* undergo a progressive reduction in length and basal body number, accompanied by a change in cell shape that becomes less tapered at the poles. The same

Table III. Split-pair Experiment

Crosses	No. of split pairs	No. of clones studied	Cell shape	No. of cells	Actively feeding cells
					%
sm19, mtVII × sm19, mtVIII	29	58	m 58 WT 0	1-60	0
WT, mtVII × sm19, mtVIII	30	60	m 12 WT 30 m + WT 18	1-60 500 500	0 100 50
sm2, mtVII × WT, mtVIII	29	58	m 27 WT 31*	1-60 500	0 100

Each member of the split pairs (see Materials and Methods) was individually transferred to 35°C in depressions containing 1 ml of culture medium, where wild-type cells can grow for approximately nine divisions before being starved. After 48 h, each clone was examined for the following traits: cell shape (either mutant [mt], or wild type [WT], see Fig. 3), growth, and feeding activity determined after 30 min of India ink ingestion. Under these conditions, all wild-type cells contain more than seven to eight large, strongly labeled food vacuoles, while mutant cells contain at most a few small and poorly labeled vacuoles. For each cross, we indicate the number of clones of homogeneous m or WT shape or of mixed m + WT shapes, the approximative number of cells per clone, and the percentage of cells actively feeding, i.e., containing more than seven to eight large food vacuoles.

* The fully wild-type phenotype of 31 clones issued from 29 split pairs can be explained by assuming that two of the pairs were actually WT × WT pairs, due to the known occurrence of some spontaneous change in mating type among wild-type populations of mating type VIII, leading to some intraclonal mating or selfing (38).

defects are produced by another nonallelic mutation, *sm2* (26). However, the physiological and ultrastructural effects of the two mutations are different. Within the limits of our observations, and in contrast to the *sm2* mutation, the *sml9* mutation bears on basal body duplication. This conclusion is supported by the following converging arguments. *sml9* cells have the same generation time as wild-type cells at 35°C (which is not the case for *sm2* cells). Protein synthesis proceeds at a normal rate, at least for the first two to three divisions, i.e., as long as the *sml9* cells can feed. The organization of all other microtubule arrays is normal and the ultrastructure of the cytoplasm (abnormal in *sm2* cells) is not affected, although parasomal sacs and trichocysts can be found at erratic locations as a result of their excess with respect to the number of basal bodies. The only ultrastructural defect observed is a rare but most often precisely located absence of one or more microtubules among the triplets of basal bodies or the outer doublets of cilia. That this particular abnormality is not a side effect of basal body underduplication is shown by the fact that it was never observed in a comparable sample of thin sections of *sm2* cells. In *sml9* cells, the temperature-sensitive period precisely corresponds to that of basal body duplication, which is not the case for *sm2* cells. Finally, the *sml9* mutational defect, but not that caused by the *sm2* mutation, can be transiently repaired by wild-type cytoplasm and more precisely by a diffusible proteinic component.

These observations lead to two conclusions. (*a*) The primary effect of the *sml9* mutation bears on an early step in basal body duplication, while the *sm2* mutation seems to affect, directly or indirectly, membrane traffic and/or biosynthesis, leading secondarily to reduced possibilities of insertion of newly formed basal bodies in the plasma membrane, as also suggested by Jones and Berger (26). (*b*) The other common properties of *sml9* and *sm2* cells, namely progressively reduced length and rounded shape, are the consequences of the reduced basal body number.

Although our data only provide circumstantial evidence, these conclusions open up interesting insights into the mechanism of basal body duplication and into the role of basal bodies in the control of the cell cycle and in the determination of cell shape in *Paramecium*.

Basal Body Duplication

The mutational defect in *sml9* cells results in the fact that daughter cells contain fewer basal bodies than their mother, and in the rare (3%) but significant occurrence of abnormal basal bodies.

The similarity of the defect observed in basal bodies and cilia indicates that the anomaly, when observed in cross sections of cilia, reflects a primary defect in their basal body. In *Paramecium*, the polarity of basal bodies (marked by their associated structures, kinetodesmal fibers, transverse and post ciliary microtubules) can be unambiguously determined in most thin sections. As previously pointed out, the missing microtubule(s) most often correspond to the site where, according to Dippell (12), the first tubule of the initial ring of nine singlets appears (see Fig. 9). However, Dippell's data do not establish whether this site is an obligate or only a preferential starting point. In the latter case, all the data can be explained by the following assumption. The defective step lies in the initiation of basal body assembly and not in basal body development, since the mutation either prevents the duplication of a basal body or slightly disturbs the earliest step in duplication without any further effect on development, once it has been initiated.

Moreover, the properties of the mutant *sml9* indicate that basal bodies assembled at the nonpermissive temperature are neither defective in their intrinsic capacity to duplicate nor in their aptitude to nucleate associated structures. First, even after several divisions at 35°C, all the basal bodies continue to nucleate normal kinetodesmal fibers, and transverse and postciliary microtubules and axonemes. Second, upon transfer back to 28°C, all basal bodies duplicate, as demonstrated by the fact that a normal spacing between basal bodies is recovered after the first division at the permissive temperature. Third, the kinetics of loss of basal bodies over successive divisions at 35°C fits the hypothesis that all basal bodies, whether previously formed at 28°C or developed at 35°C, display the same probability (~60%) of duplication and maintain it over successive divisions at 35°C. If basal bodies formed at 35°C were unable to duplicate, their kinetics of loss over the first three divisions would be much steeper; 51, 35, and 22 instead of the observed values of 51, 41, and 32 (Table I). Finally, we have shown that the mutational defect can be repaired by microinjection of wild-type cytoplasm and that this effect, although transient, lasts for at least three to four cell generations. This renders unlikely the hypothesis that the mutated factor is a structural component of the basal body itself or of its associated pericentriolar-like material.

It is worth pointing out that the *sml9* mutation is the first one known to affect the initiation of basal body duplication. The earliest mutation so far reported is the *bald 2* mutation in *Chlamydomonas* (17), which blocks basal body development beyond assembly of the initial ring of nine singlet microtubules. In view of the numerous mutations affecting flagellar assembly obtained in *Chlamydomonas* (20–22, 32) and in *Physarum* (34), and the various screening methods used to isolate flagellar mutants in these organisms, it seems surprising that no mutant unable to duplicate basal bodies has been described. The absence of such mutants can be interpreted in two ways: either such mutations are immediately lethal or very few genes are involved in the process. Immediate lethality would indicate that these genes perform crucial functions other than basal body duplication. This does not seem to be the case for the *sml9* mutation.

Altogether, the data suggest that the gene *sml9*$^+$ codes for a product, specifically necessary for basal body duplication and not required for the development and properties of the structure itself. Kuriyama and Borisy (29) have also reported evidence for a specific duplication signal in the centriole cycle of Chinese hamster ovary cells. In *Paramecium*, the restoration of the mutational defect by microinjection of wild-type cytoplasm into *sml9* cells opens up the possibility of characterizing the duplication factor.

In any case, the original defect observed in the organization of some *sml9* basal bodies provides new information on basal body biogenesis. First, the assembly of the nine initial microtubules is not interdependent. Second, the overall ninefold symmetry of the basal body is not disturbed by the absence of a triplet of microtubules, and therefore appears prepatterned in the germinative disc.

Basal Bodies, Cell Cycle, Cell Size, and Cell Shape

The cycle of basal bodies, like that of centrioles (29) is strictly coupled to the cell cycle. However, cells can divide without centrioles, as shown in *Drosophila* (10), or divide normally regardless of the number of their basal bodies, as already observed in *Chlamydomonas* (42) and *Euplotes* (14). The fact that *sml9* cells continue to divide at a normal rate while their basal body number decreases confirms that this parameter is not involved in the control of the cell cycle. Basal body duplication would therefore appear as a terminal and dispensable process. However, in *Paramecium*, the reduction in the number of basal bodies results in a change in cell shape (without notable change in cell mass, at least in the short run, as long as the cells can feed). This change, most easily measured in terms of cell length, leads first to less tapered cells and then to ovoid ones. The simplest interpretation of these observations is that the normal shape of *Paramecium* is partly determined by the physical constraints exerted over its cortex by the basal bodies and their associated structures (kinetodesmal fibers, and transverse and postciliary microtubules), which form a dense and rigid cortical network. As the density of basal bodies decreases faster than cell length, the shape of the cell becomes less constrained. It is interesting to note that, at least in the short run (first two to three divisions), this change in the shape of the cell does not affect its overall metabolism, since in particular protein synthesis seems unaffected and cell length decreases much less than basal body number, resulting in a wider basal body spacing. However, by the third division, basal body spacing ceases to decrease, while both basal body total number and cell length continue to do so (see Table I). These observations suggest, although they do not demonstrate, that basal body number might be coupled to cell metabolism, in agreement with results on *Tetrahymena* (35) showing that it is the total number of basal bodies that is constant rather than their arrangement.

Finally, it can be pointed out that, despite reduction in basal body number, the secondary disorganization of cortical units, and change in cell shape, the overall cortical pattern is not notably modified, in agreement with other results showing that, in *Tetrahymena* (13), pattern and cell shape are largely independent and that, in *Pleurotrycha lanceolata* (18) and *Paraurostyla weissei* (23), pattern and assembly of basal body–associated structures are not interdependent.

In the cortex of ciliates, basal bodies would therefore primarily respond to diffusible or structural signals for duplication and patterning but would also in turn contribute to the determination of cell shape and cortical pattern.

We wish to thank Dr. Linda Sperling for her stimulating interest in this work and critical reading of the manuscript, Dr. Jean Cohen for many helpful suggestions and Dr. André Adoutte and Dr. Michel Bornens for discussions.

This work was supported by grants from the Centre National de la Recherche Scientifique and from the Ligne Nationale Française contre le Cancer.

Received for publication 15 April 1986, and in revised form 5 October 1986.

References

1. Aufderheide, K. 1978. The effective site of some mutations affecting exocytosis in *Paramecium tetraurelia*. *Mol. & Gen. Genet.* 165:199–205.

2. Beisson, J., and T. M. Sonneborn. 1965. Cytoplasmic inheritance of the organization of the cell cortex in *Paramecium aurelia*. *Proc. Natl. Acad. Sci. USA.* 53:275–278.

3. Beisson, J., J. Cohen, M. Lefort-Tran, M. Pouphile, M. Rossignol. 1980. Control of membrane fusion in exocytosis: physiological studies on a *Paramecium* mutant blocked in the final step of trichocyst extrusion process. *J. Cell Biol.* 85:213–227.

4. Berger, J. D. 1976. Gene expression and phenotypic change in *Paramecium tetraurelia* exconjugants. *Genet. Res.* 27:123–134.

5. Berger, J. D. 1984. The ciliate cell cycle. *In* The Microbial Cell Cycle. P. Nurse and E. Streiblova, editors. CRC Press Inc., Boca Raton, Florida. 191–208.

6. Berger, J. D., and C. Pollock. 1981. Kinetics of food vacuole accumulation and loss in *Paramecium tetraurelia*. *Trans. Am. Microsc. Soc.* 100:120–123.

7. Chatton, E., and A. Lwoff. 1936. Techniques pour l'étude des Protozoaires, spécialement de leurs structures superficielles (cinetome et argyrome). *Bull. Soc. Fr. Microsc.* 5:25–39.

8. Cohen, J., and J. Beisson. 1980. Genetic analysis of the relationships between the cell surface and the nuclei in *Paramecium tetraurelia*. *Genetics.* 95:797–818.

9. Cohen, J., A. Adoutte, S. Granchamp, L. M. Houdebine, and J. Beisson. 1982. Immunocytochemical study of microtubular structures throughout the cell cycle of *Paramecium*. *Biol. Cell.* 44:35–44.

10. Debec, A., A. Szöllösi, and D. Szöllösi. 1982. A *Drosophila melanogaster* cell line lacking centrioles. *Biol. Cell.* 44:133–138.

11. Dippell, R. 1955. A temporary stain for *Paramecium* and other protozoa. *Stain Technol.* 30:60–71.

12. Dippell, R. V. 1968. The development of basal bodies in *Paramecium*. *Proc. Natl. Acad. Sci. USA.* 61:461–468.

13. Doerder, F. P., J. Frankel, M. Jenkins, and L. E. Deboult. 1975. Form and pattern in ciliated protozoa: analysis of genic mutant with altered cell shape in *Tetrahymena pyriformis*, syngen 1. *J. Exp. Zool.* 192:237–258.

14. Frankel, J. 1973. A genetically determined abnormality in the number and arrangement of basal bodies in a Ciliate. *Dev. Biol.* 30:336–365.

15. Fukushi, T., and K. Hiwatashi. 1970. Preparation of mating reactive cilia from *Paramecium caudatum* by $MnCl_2$. *J. Protozool.* 17:(Suppl.) 21. (Abstr.)

16. Giloh, M., and J. W. Sedat. 1982. Fluorescence microscopy: reduced photobleaching of rhodamine and fluorescein protein conjugates by n-propyl gallate. *Science (Wash. DC).* 21:1252–1255.

17. Goodenough, U. W., and H. Sheldon St. Clair. 1975. Bald-2: a mutation affecting the formation of doublet and triplet sets of microtubules in *Chlamydomonas reinhardii*. *J. Cell Biol.* 66:480–491.

18. Grimes, G. W., M. E. Mc Kenna, C. M. Goldsmith-Spoegleer, and A. Knaupp. 1980. Patterning and assembly of ciliature are independent processes in Hypotrich Ciliates. *Science (Wash. DC).* 209:281–283.

19. Hiwatashi, K., N. Haga, and M. Takhashi. 1980. Restoration of membrane excitability in a behavioral mutant of *P. caudatum* during conjugation and by microinjection of wild type cytoplasmic factor. *J. Cell Biol.* 84:476–480.

20. Huang, B., M. R. Rifki, and D. J. L. Luck. 1977. Temperature sensitive mutations affecting flagellar assembly and functions in *Chlamydomonas reinhardtii*. *J. Cell Biol.* 72:67–85.

21. Huang, B., Z. Ramanis, S. K. Dutcher, and D. J. L. Luck. 1982. Uniflagellar mutants of *Chlamydomonas*: evidence for the role of basal bodies in transmission of positional information. *Cell.* 29:745–753.

22. Jarwick, J. W., and B. Chojnacki. 1985. Flagellar morphology in stumpy-flagella mutants of *Chlamydomonas reinhardtii*. *J. Protozool.* 32:649–656.

23. Jerka-Dziadosz, M. 1983. The origin of mirror-image symmetry doublet cells in the Hypotrich Ciliate *Paraurostyla weissei*. *Roux's Arch. Dev. Biol.* 192:179–188.

24. Jones, W. R. 1976. Oral morphogenesis during asexual reproduction in *Paramecium tetraurelia*. *Genet. Res.* 27:105–117.

25. Jones, D. 1977. Mutational analysis of cell development in *Paramecium tetraurelia*. Ph.D. thesis. University of British Columbia, Vancouver, British Columbia, Canada. 289 pp.

26. Jones, D., and J. D. Berger. 1982. Temperature sensitive mutants affecting cortical morphogenesis and cell division in *Paramecium tetraurelia*. *Can. J. Zool.* 60:2296–2312.

27. Kaneda, M., and E. D. Hanson. 1974. Growth patterns and morphogenetic events in the cell cycle of *Paramecium aurelia*. *In* Paramecium: A Current Survey. W. J. van Wagtendonk, editor. Elsevier Publishing Co., Inc., New York. 219–262.

28. Knowles, J. K. C. 1974. An improved microinjection technique in *Paramecium aurelia*. *Exp. Cell Res.* 88:79–87.

29. Kuriyama, R., and G. G. Borisy. 1981. Centriole cycle in Chinese hamster ovary cells as determined by whole mount electron microscopy. *J. Cell Biol.* 91:814–821.

30. Lowry, O. H., N. J. Roseborough, A. L. Farr, and R. J. Randall. 1951. Protein measurement with the Folin phenol reagent. *J. Biol. Chem.* 193:265–275.

31. Mc Donald, B. 1966. The exchange of RNA and protein during conjugation in *Tetrahymena*. *J. Protozool.* 13:277–285.

32. Mc Vittie, A. 1972. Flagellum less mutants of *Chlamydomonas reinhardtii*. *J. Gen. Microbiol.* 71:525–540.

33. Mazia, D., G. Schatten, and W. Sale. 1975. Adhesion of cells to surfaces coated with polylysine. *J. Cell Biol.* 66:198–200.

34. Mir, L., L. Delcastillo, and M. Wright. 1979. Isolation of *Physarum*

amoebal mutants defective in flagellation and associated morphogenetic processes. *FEMS (Fed. Eur. Microbiol. Soc.) Microbiol. Lett.* 5:43–46.

35. Nanney, D. L., and M. C. Chow. 1974. Basal body homeostasis in *Tetrahymena*. *Am. Nat.* 108:125–129.

36. Ogura, A. 1977. Non-lethal deciliation of *Paramecium* with ethanol. M. S. thesis. University of Tokyo, Tokyo, Japan.

37. Schliwa, M., and J. Van Blerkom. 1981. Structural interaction of cytoskeletal components. *J. Cell Biol.* 90:222–235.

38. Sonneborn, T. M. 1970. Methods in *Paramecium* research. *Methods Cell Physiol.* 4:241–339.

39. Sonneborn, T. M. 1970. The *Paramecium aurelia* complex of fourteen sibling species. *Trans. Am. Microsc. Soc.* 94:155–178.

40. Sonneborn, T. M. 1974. Handbook of Genetics. Vol. 2. R. C. King, editor. Plenum Publishing Corp., New York. 469–594.

41. Whitson, G. L. 1964. Temperature sensitivity and its relation to changes in growth, control of cell division, and stability of morphogenesis in *Paramecium aurelia*, syngen 4, stock 51. *J. Cell. Comp. Physiol.* 64:455–465.

42. Wright, R. L., B. Chojnacki, and J. W. Jarvik. 1983. Abnormal basal body number location and orientation in a striated fiber defective mutant of *Chlamydomonas reinhardtii*. *J. Cell Biol.* 96:1697–1707.